25 nm mechanically buttressed high aspect ratio zone plates: Fabrication and performance

Deirdre L. Olynick,[a] Bruce D. Harteneck, Eugene Veklerov, Mihir Tendulkar, and J. Alexander Liddle
Center for X-Ray Optics, Lawrence Berkeley National Laboratory, Berkeley, California

A. L. David Kilcoyne
Advanced Light Source, Lawrence Berkeley National Laboratory, Berkeley, California

Tolek Tyliszczak
Chemical Sciences Division, Lawrence Berkeley National Laboratory, Berkeley, California

(Received 3 June 2004; accepted 20 September 2004; published 10 December 2004)

High performance zone plates are critical for advancing the state-of-the-art in x-ray microscopy, both in terms of spatial and energy resolution. Improved resolution, increased energy bandwidth, and enhanced efficiency can be achieved through the fabrication of smaller, higher aspect ratio outer zones. Using electron beam lithography, we have fabricated and obtained initial performance data from a 25 nm outer zone width zone plate, with a 7:1 aspect ratio, using a hydrogen silsesquioxane (HSQ)/cross-linked polymer bilayer process. We investigated the effectiveness of buttresses, i.e., mechanical supports perpendicular to the zones, on our ability to achieve higher aspect ratios which conventionally would be unreachable due to resist collapse. Optimum buttress spacing is affected by film thickness, linewidth, collapse mechanisms, and resist modulus. For 25 nm zones, etched into 150 nm cross-linked polymer (AZPN114), buttress spacings of approximately two times the resist thickness or ten times the zone width are sufficient to prevent collapse during plating. We find that high aspect ratio features not only have to be able to withstand collapse during liquid immersion, but also during dry etching processes. In addition, we show that a 50% feature bias and longer development times (8 min in 1% TMAH based solutions) allow smaller dense feature sizes by eliminating resist webbing frequently observed in electron-beam imaging of HSQ. © *2004 American Vacuum Society.* [DOI: 10.1116/1.1815298]

I. INTRODUCTION

Zone plates are still the most practical and useful structures for focusing x rays for the purposes of microscopy. The best zone plates have a demonstrated resolution of 20 nm, corresponding to an outer zone width of 25 nm.[1] However, these zone plates, with aspect ratios of approximately 2:1, are useful only up to energies of 900 eV. In addition, even at lower energies, aspect-ratio limited, i.e., thickness limited, focusing efficiency requires longer exposure times which increases damage to radiation sensitive materials. In order to work at higher energies, where many more elements are accessible spectroscopically, and with greater efficiency, it is necessary to fabricate high aspect ratio zone plates.

Previous work has shown that there is a critical aspect ratio for collapse of resist features exposed to a liquid that limits the aspect ratios that can be successfully patterned for features of arbitrary length.[2,3] To avoid resist collapse during development, bilayer schemes, where a thin imaging layer is transferred with a plasma etch into a relatively thick underlayer, are used. However, when the actual zone plate is formed by electroplating metal between the remaining resist features, regardless of the initial patterning process, high aspect ratio features must survive immersion in a liquid.

It is possible in the case of zone plates, to buttress the zones with additional features to form mechanical support structures. These buttressed structures can have significantly higher resistance to collapse without seriously compromising the zone plate performance. Ideally, optimum buttress structures should use a minimum of real estate for mechanical support but maximize the resistance to collapse.

In this article, we detail the fabrication and show initial high energy performance results for a buttressed 25 nm, 7:1 aspect ratio outer zone width zone plate using a HSQ/cross-linked AZPN114 bilayer scheme. We investigate optimum buttress structures and find that for 25 nm zones, etched into 150 nm AZPN114, the optimum buttress spacing is close to ten times the zone width. Our cryogenic etching studies show that profile control is crucial and that the dry etching process itself can also lead to structure collapse. In addition, we show that feature bias and longer development time can eliminate the resist webbing frequently observed in electron e-beam imaging of HSQ. This also improves our ability to generate small, high aspect ratio structures.

II. EXPERIMENT

The goal for our zone plate was to be able to work from 300 eV to over 1 keV with high resolution, good efficiency, and large focal lengths. The specific zone plate parameters were: diameter=120 μm, number of zones=1200, outer

[a]Author to whom correspondence should be addressed; electronic mail: dlolynick@lbl.gov

zone width=25 nm, and nominal operating wavelength =2.07 nm (600 eV). The optimum efficiency at 600 eV was achieved at a zone plate thickness between 180 and 200 nm.

We have discussed the fabrication of diffractive optics using a HSQ/cross-linked AZPN114 bilayer process, cryogenic etching, and plating previously.[4] Only the changes are noted here.

A plating base of 5 nm Cr and 10–12 nm of Au was formed on the membrane wafers using e-beam evaporation. Wafers were coated with a 30% weight solution of Sumitomo AZPN114 photoresist and hardbaked at 250 °C for 5 min producing a 180 nm film. Next, a 1.8% solution of HSQ (Fox-15, Dow Corning, 18% solids) was spun at 4000 rpm, oven baked for 5 min on a copper plate at 170 °C for 30 min, producing a film of approximately 30 nm thickness.

The zone plate resist pattern was exposed in HSQ using a modified[5] Leica VB6HR at 100 keV with 450 pA beam current and a 10 nm spot size. Lines were printed at a 1:1 line to space ratio with a 50% negative bias. Optimum 25 nm zone plate doses were approximately 2500 $\mu C/cm^2$. The wafers were developed in 100% Shipley LDD 26-W for 8 min, rinsed in de-ionized (DI) water and blown dry.

The AZPN114 was etched for 75 s in an Oxford Plasmalab 100 ICP 380 etcher at cryogenic temperatures. After etching, wafers were warmed to room temperature, under vacuum, to prevent water condensation on the cold wafers and possible resist collapse.

After etching, the wafers were plated with Au to a thickness of 175 nm using sodium aurosulfite from Enthone-OMI at 45 °C and a current density of 1.3 mA/cm^2. This results in a plating rate of about 100 nm/min. The plating rate was optimized to give the lowest stress and suitably small grains.

A second e-beam lithography step was used to plate the open areas of the SiN_4 support membrane inside (central stop) and outside the zone plate to reduce stray background and zero order light in the x-ray microscope. AZPN114 100% was spun as a negative e-beam resist at 2000 rpm, and postapply baked at 120 °C for 2 min. The resist was exposed at 188 $\mu C/cm^2$, postexposure baked at 105 °C for 5 min, and developed for 60 s in Shipley Corp. MF-312. The open membrane areas were then gold electroplated to a thickness of 1 μm.

For buttressed resist collapse tests, a bilayer film of 100 nm HSQ and 200 nm cross-linked AZPN114 was produced. Collapse was studied after development (HSQ collapse) and after dry etching to a depth of 100 and 200 nm into the cross-linked resist. Three buttressed line structures were investigated: grid [Fig. 1(a)], brick [Fig. 1(b)], and railroad [Fig. 1(c)] and compared to unbuttressed lines of the same spacing and resist. The goal was to minimize buttress real estate (area fraction) and maximize line stability. Spacings analyzed were 20, 13, 10, and 8 times the linewidths.

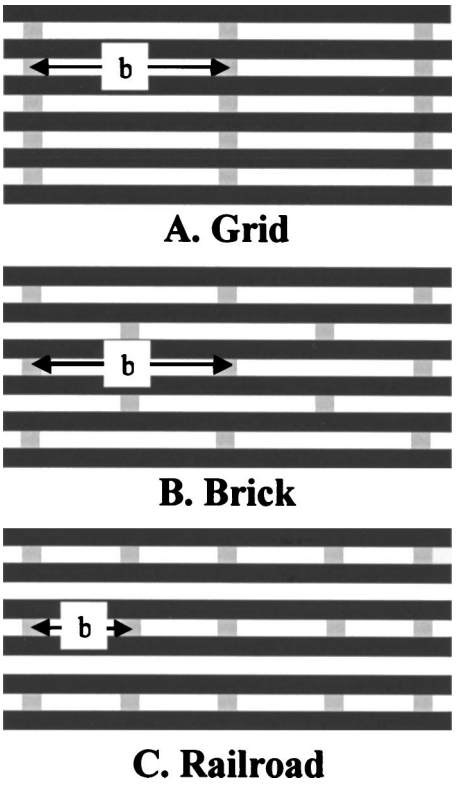

FIG. 1. Schematic of buttress structures. Spacing between buttresses is *b*.

III. RESULTS AND DISCUSSION

A. Effect of bias and development time

Previously, we have shown that with HSQ and shorter development times, the bias improves process latitude but decreases dose sensitivity.[6] We have found that a critical issue for dense features produced in HSQ is the onset of webbing or microbridging of features. This webbing forms random unwanted connections between lines and increases in severity as the dose to print on size is approached and exceeded. In addition to producing unwanted features, webbing must be avoided as it causes line displacement [see for example Fig. 2(a)].

Figure 2 shows the combined effects of longer development time and bias. The dose for the onset of webbing is circled with the accompanying scanning electron microscopy (SEM) micrograph shown (a and b). The lower slope of the biased lines shows that the combination of bias and longer development time produces the expected increase in process latitude. As the HSQ dose-to-print can have poor reproducibility,[4,7] this increased process latitude is especially important. One consequence of line biasing is decreased linewidth uniformity between lines on the outside of the pattern and lines on the inside. As a consequence, the thinner lines in Fig. 3(b) have collapsed. We discuss line collapse mechanisms in the subsequent section.

B. Line collapse and buttresses

Resist line collapse was first studied by Tanaka *et al.*[3] As features dry after development, unbalanced capillary forces

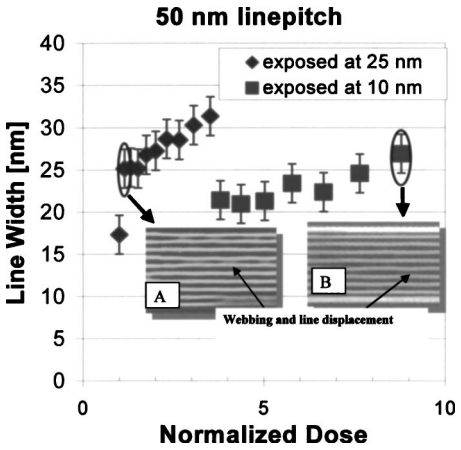

FIG. 2. Linewidth vs dose for 50 nm pitch lines. Biased lines (b) have more process latitude.

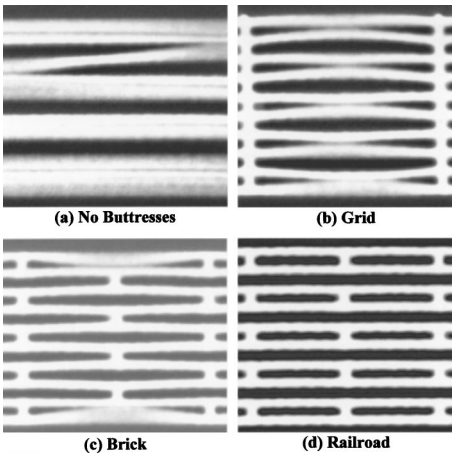

FIG. 4. Unbuttressed vs buttressed 23 nm lines at 60 nm pitch in 100-nm-thick HSQ. Buttresses spacing is six times the resist thickness.

produce a differential pressure. For equal lines and spaces, areas filled with liquid have less pressure than areas that are already dry. This pressure difference is given from the Laplace equation as

$$\Delta P = \frac{2\gamma \cos\theta}{S}, \tag{1}$$

where γ is the surface tension between the solvent and gas phase, S is the distance between neighboring lines (the capillary width), and θ is the angle the surface tension vector makes with the resist.

For elastic collapse, failure occurs when the resist elastically bends far enough to touch a neighboring structure and stick. In the small angle elastic deflection regime (truly valid only for deflection-to-resist-height ratios less than 0.2, but valid within an order of magnitude for deflections up to 0.8),[8] the pressure needed to achieve a given deflection of a resist feature modeled as a cantilever beam is

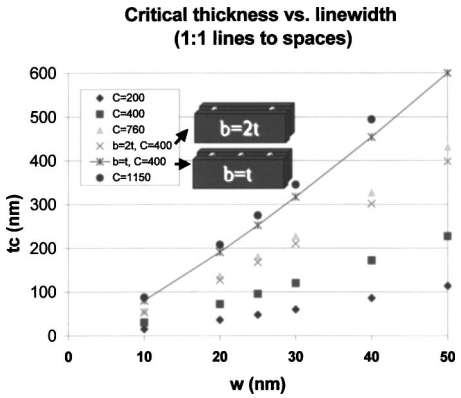

FIG. 3. Critical thickness of collapse vs w (linewidth) for collapse due to liquid immersion. C represents the properties of the collapsing material and the liquid/material interface. Above the critical thickness lines will collapse. Curves connected with lines are for buttressed structures. Higher thickness structures can be reached with buttressed lines with the same C.

$$P_b = \frac{q}{D} = \frac{2\partial_b E w^3}{3t^4}, \tag{2}$$

where P_b is the bending pressure required to achieve a deflection of ∂_b, q is a bending force per unit length, D is the length of the zone or line, E is Young's modulus, w is the linewidth, and t is the resist thickness.

If the bending pressure is a result of meniscal forces, then $q/D = 2\gamma\cos\theta/S$, from Eq. (1). For simplicity, we do not take into account the bending pressure dependence on resist deflection as analyzed by Tanaka *et al.*[3] Setting $S=w$, (1:1 line-to-space ratio) and $\partial_b = w$ (one line collapses while the other remains erect), the critical collapse thickness is

$$t_c = 0.33^{1/4} C w^{5/4}, \tag{3}$$

where $C = (E/\gamma\cos\theta)^{1/4}$.

We model buttressed lines as simply supported plates at the buttresses, built-in at the bottom (the resist/substrate interface) and free at the top edge. The solution to the problem for a small angle deflections and a Poisson ratio of 0.33 is found in Ref. 9. The critical dependency in this model is the resist thickness (t) to buttress spacing (b) ratio, t/b. For t/b values of <1, the structure acts similarly to a cantilever beam [Eq. (3)] with a correction factor related to the Poisson ratio and the t/b ratio. As the t/b ratio approaches 3 (thick resists with more closely spaced buttresses), the effect of the built-in support at the resist-substrate interface becomes insignificant, and the resist system acts like a beam simply supported on both ends with a support spacing equivalent to the buttress spacing. In this regime, the collapse becomes independent of resist thickness and is dependent only on the buttress spacing and linewidth. In theory, one could reach indefinite aspect ratios with the only drawback being the loss in real estate from the closely spaced buttresses.

In Fig. 3, we plot the critical resist thickness as a function of linewidth for 1:1 lines and spaces using the simple cantilever model (unbuttressed lines), and the plate model (buttressed lines). At constant resist thickness, the buttress spacing must decrease to prevent collapse as w (linewidth) is

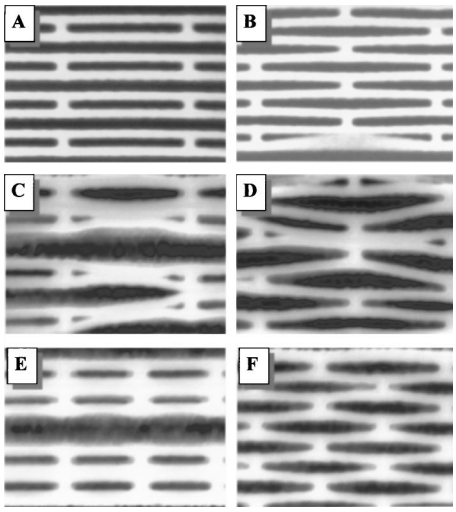

FIG. 5. Effect of bilayer etching on 30 nm buttressed lines. (a) No etching, railroad, $b=6t$. (b) No etching, brick. (c)–(f) Oxygen cryoetch, 2 min (total structure thickness=300 nm). (c) Railroad, $b=2h$. (d) Brick, $b=2t$. (e) Railroad, $b=0.4t$, (f) Brick, $b=0.5t$. Small spacing brick structures can withstand collapse after etching.

reduced (until t/b is greater than 3 when collapse becomes independent of film thickness). To achieve an uncollapsed 167 nm structure (approximately our zone plate height) after liquid immersion, a nonbuttressed structure would have to have a Young's modulus ten times greater than that of a buttressed structure (with $b=2t$, buttress spacing twice the resist thickness). For a water to air interface ($g=72.8$ mPa), and a perfectly wetting material ($\theta=0$), this would require an increase in Young's modulus from 2 to 20 GPa. Even using this simple order of magnitude calculations, it becomes obvious that buttresses provide a means of increasing the aspect ratios far beyond what can be reached even with very heavily cross-linked resists [poly(methyl methacrylate) heavily cross-linked approaches an acrylic structure with a modulus

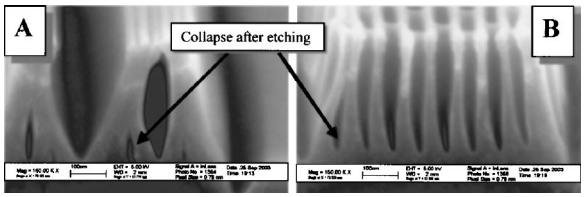

FIG. 6. Cross-section of 40 nm bilayer lines. Total height is approximately 330 nm.

on the order of 4 GPa].[10] Thus buttresses are an excellent alternative to using very high modulus materials.

Figure 4 compares unbuttressed lines with grid, brick, and railroad buttressed structures for 23 nm lines and 60 nm pitch in a 100 nm film of HSQ. Buttressed brick and railroad structures were mostly uncollapsed at buttress spacings six times the resist thickness. (This translates to an unsupported line width 20 times the resist spacing, and 5% area fraction.) Grid buttresses collapsed because the effective buttress spacing is twice that of the railroad and brick types (same buttress area fraction).

In Fig. 4(c) there is some bowing of the resist lines. We saw the uncoated lines bowing as we imaged the samples with the SEM and were able to discern with subsequent tests of gold coated samples that samples were not bowed before SEM imaging. Figure 5 shows that the 30 nm wide buttressed lines are stable after development [5(a) and 5(b)], but fall over after 2 min of etching into the AZPN114 [5(c) and 5(d), total HSQ+AZ structure height of 280 nm]. For the range of buttress spacings we studied, reducing the buttress spacing mitigates the problem for the brick structure [5(f)] but not for the railroad structure [5(e)]. At some point the line pairs in the railroad structure will act like single, unbuttressed lines.

The mechanism of collapse during the dry etching step is still unclear. From the cross section images shown in Fig. 6,

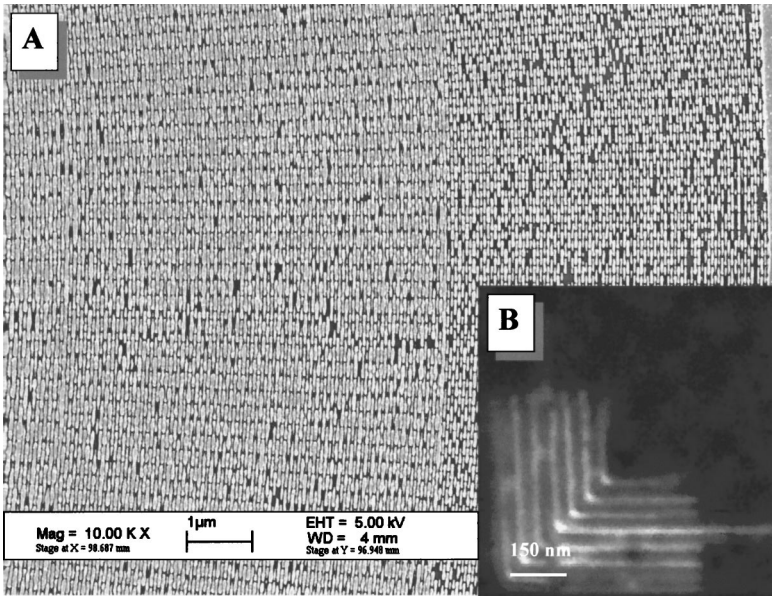

FIG. 7. (a) Zone plate outerzones. (b) x-ray microscope image using zoneplate. Line pitch of elbow is 50 nm.

it is obvious that collapse occurs after the etching process: the individual lines are etched to the same depth but have fallen together. Possibly, collapse occurs upon warm-up of the cryogenic etching due to differential thermal expansion. Another possibility is that charging of the resist by the plasma during etching pulls the lines together. We will investigate this further in the future.

Figure 7(a) shows the outer region of the 25 nm outer zone width gold electroplated brick buttressed zone plate (50% biased lines, long development times). Only the outer 15 μm are buttressed and the buttress area fraction is approximately 10%. Figure 7(b) shows an x-ray microscope image[11] of a 25 nm linewidth/50 nm pitch elbow pattern using this zone plate. These initial measurements, taken at 350 eV, indicate a working high resolution, buttressed zone plate. Initial efficiency measurements are slightly lower than theoretically predicted as the plated outerzone linewidths are oversized (caused by underexposure of the resist).

IV. CONCLUSIONS

We have analyzed the performance of three buttressed structures at various line widths and three resist thicknesses. Brick buttressed structures were optimum due to the higher mechanical strength (both after liquid immersion and etching) at the lowest area fraction. With a simplified theoretical model of collapse, we have shown that buttresses offer the possibility of manufacturing very high aspect ratio structures with unlimited aspect ratios once the resist thickness to buttress spacing ratio approaches a value of 3. The only drawback is the loss of real estate. For zone plates, this loss of real estate translates to a reduction in zone plate transmission (less brightness in the central spot). Furthermore, we observed that resist collapse can occur as a result of plasma processing. Although the exact mechanism is still unclear, buttresses were also able to mitigate this collapse.

Using a brick buttress system, 50% biased lines, and long development times, we have fabricated a 7:1 aspect ratio gold-electroplated zone plate which is able to resolve 1:1 lines and spaces at a 25 nm linewidth over a wide range of x-ray energies. This is the first step to achieving even higher resolution, higher efficiency zone plates. We expect this technique to find applications in microelectromechanical systems and certain microelectronic structures.

[1]W. Chao *et al.*, Opt. Lett. **28**, 2019 (2003).
[2]H. B. Cao, P. F. Nealey, and W. D. Domke, J. Vac. Sci. Technol. B **18**, 3303 (2000).
[3]T. Tanaka, M. Morigami, and N. Atoda, Jpn. J. Appl. Phys., Part 1 **32**, 6059 (1993).
[4]D. L. Olynick *et al.*, J. Vac. Sci. Technol. B **19**, 2896 (2001).
[5]E. H. Anderson, V. Boegli, and L. P. Muray, J. Vac. Sci. Technol. B **13**, 2529 (1995).
[6]E. H. Anderson *et al.*, J. Vac. Sci. Technol. B **19**, 2504 (2001).
[7]W. Henschel, Y. M. Georgiev, and H. Kurz, J. Vac. Sci. Technol. B **21**, 2018 (2003).
[8]J. M. Gere and S. Timoshenko, *Mechanics of Materials* (PWS-KENT, Boston, 1990).
[9]S. Timoshenko, *Theory of Plates and Shells* (McGraw-Hill, New York, 1959).
[10]http://www.salemball.com/acrylic.htm
[11]A. L. D. Kilcoyne *et al.*, J. Synchrotron Radiat. **10**, 125 (2003).